RESEARCH ARTICLE

Video Refereeing Model of Soccer Match Based on Fuzzy Clustering and Cuckoo Optimization Algorithm

TING WANG¹, JINGLONG GENG², JING WANG³, AND XIAO YAN¹
¹Physical Education College, Shanxi University, Taiyuan 030006, China
²Physical Education College, Taiyuan Normal University, Jinzhong 030619, China
³Physical Education College, Shanxi Vocational University of Engineering Science and Technology, Jinzhong 030619, China

Corresponding author: Jinglong Geng (gengjinglong2022@126.com)

ABSTRACT Computer technology has rapidly advanced the use of computer-assisted refereeing in sports. However, motion image segmentation presents several challenges, including image blurring due to high-speed motion and the impact of ambient light on image accuracy. These challenges can affect the referee's judgment of the game. To address this issue, the research utilizes sinusoidal mapping and the simplex method to enhance the cuckoo algorithm. Additionally, the optimization accuracy is improved through sinusoidal adaptive discovery probability. To tackle the problem of the fuzzy clustering algorithm's weak global search ability, the clustering center is optimized by enhancing the cuckoo algorithm. To optimize the objective function, domain space information is introduced into the fuzzy clustering algorithm to address its sensitivity to noise. As the number of iterations approached 500, the experimental findings showed that the convergence accuracy of the particle swarm algorithm, the sparrow algorithm, the modified cuckoo algorithm, and the cuckoo algorithm were, respectively, 0.99, 0.89, 0.85, and 0.73. The enhanced algorithm model, enhanced cuckoo-fuzzy C-mean algorithm model, cuckoo-fuzzy C-mean algorithm model, and fuzzy C-mean algorithm model had delineation effects of 0.80, 0.72, 0.70, and 0.61, in that order. The outcomes show that the suggested algorithm can more accurately segment images from soccer matches. This provides a valuable reference for future computer-assisted match discrimination.

INDEX TERMS Image segmentation, fuzzy clustering, cuckoo's algorithm, match discrimination, sine mapping.

I. INTRODUCTION

In recent years, computer technology has advanced significantly, and video and images have become essential tools for interacting with information. The benefits of using video and images are their ease of comprehension and ability to convey a large amount of information. Therefore, images are crucial for effective information transfer [1]. However, not all parts of an image contain useful information, and it is necessary to extract the relevant information [2]. A heuristic optimization technique with improved convergence and global search capacity is the cuckoo optimization

algorithm (COA). To get the best answer, it mimics the foraging habits of Cuckoos. When it comes to soccer match video refereeing, the COA can adjust the FC algorithm's parameter parameters to better accommodate various match situations and penalty concerns. This research presents an improved algorithm for fuzzy clustering (FC) image segmentation (FCIS) with noise immunity, which accurately segments images in game videos.

There are three innovative points: (1) In response to the weak local search ability and fixed parameter settings of the traditional cuckoo algorithm, the model is improved. (2) The fuzzy C-means clustering algorithm has the shortcomings of being greatly affected by the initial clustering center and weak global search ability. Integrate the improved cuckoo

The associate editor coordinating the review of this manuscript and approving it for publication was Fahmi Khalifa.

algorithm with the FCM clustering algorithm. (3) To address the sensitivity of fuzzy clustering algorithms to noise, domain spatial information is introduced into the algorithm to optimize the objective function.

There are four primary sections of the paper. An overview of previous research on image segmentation (IS) algorithm modeling by various scholars is given in the first section. The second section provides a review of the primary research methods used, followed by the model results obtained by applying these methods and analyzing the outcomes in the third section. The fourth section summarizes the aforementioned studies and provides an outlook for future research.

II. RELATED WORKS

IS is an important image processing technique. M. M. Woldeamanuel et al. found that combining infrared thermography and IS can be well used for automatic estimation of concrete strength at construction sites. Therefore, the research team proposed a deep learning-based IS method to segment concrete areas in true color images using a pre-trained convolutional neural network-based model after acquiring image data. Experimental results showed that the method can estimate concrete strength in real time in an economically feasible manner and helps to optimize the formwork removal time of the structure [3]. A U-net-based IS model was proposed by J. Fan et al. to study the coal micro-components' particle morphology, size, release characteristics, and density separation process. The findings showed that the suggested method offered strong computer-assisted measurements for the logical separation and use of coal micro-components, in addition to having significant potential for qualitative analysis of micro-component composition and their release types [4]. B. Ostdiek et al. found that detecting substructures in strong lensing images is an important way to reveal the nature of dark matter. To this end, the team proposed a method to localize the subhalos in the images by neural networks and determine their quality using IS techniques. The experimental findings showed that the suggested approach may effectively segment images with significant lensing [5].

Kumar et al. argued that IS can be applied to the analysis of crops. Therefore, an entropic threshold segmentation method is proposed which finds the juja threshold of the function by CS. According to the experimental results, the suggested technique performed well when tested for accuracy on ten cropped photographs with complicated backgrounds and high-dimensional color intensity space [6]. According to G. Xiang et al., offshore activities frequently include the problem of trajectory optimization of submerged elongated entities. To address this problem, accurate prediction of the trajectory of a free-falling body is needed, combined with effective optimization algorithms to establish an optimization framework that satisfies the specific task. To accurately represent the 3D effects, the study team suggested a CS-based 3D dynamics model that accounts for the lateral forces and motions caused by axial rotation in cross-flow and

asymmetric vortex shedding. The outcomes demonstrated that the method performs better than genetic algorithms and particle swarm optimization algorithms [7]. D. K. Angura et al. found that clustering is an effective way to reduce the overall energy consumption of medical wireless devices in healthcare organizations, but the main drawback of the existing model is the sustainability of the network. To address this issue, this research proposed an evolution-based augmented bifold cuckoo search algorithm. The suggested strategy performs the model better, according to experimental data [8]. L.W. Wang et al. proposed a new deep luminescence network to solve the problem of low light image enhancement. This network utilizes the latest technology of convolutional neural networks to iteratively brighten and darken multiple LBP blocks, thereby learning the residuals of normal light estimation. To effectively integrate local and global features, adaptive feature aggregation blocks are also introduced. The experimental results indicate that DLN outperforms other methods in both objective and subjective indicators [9]. W. Zhang et al. proposed a spatial, spectral, and texture aware attention network to identify corn varieties in order to address the problem of hyper-spectral image assisted seed recognition that only considers spectral information and ignores spatial information. By utilizing the complementary properties of 3D and 2D convolutions, the spatial and texture features of hyper-spectral images are fully utilized. The experimental results indicate that SSTNet is superior to state-of-the-art methods in identifying maize varieties [10]. B. Subraman et al. proposed an optimal weighted multi-exposure histogram equalization model to improve image contrast enhancement techniques. This method divides the image into sub images and applies cropping and weighting processing to avoid excessive enhancement. By separately balancing and integrating sub histograms, maintain naturalness and detail. Using dual gamma correction to improve contrast in dark areas, and optimizing the enhancement degree using the spiral krill swarm algorithm. The experiment shows that this technology improves the visual quality of images [11]. P. Ma et al. proposed a fusion algorithm to improve the classification accuracy of brain computer interfaces based on steady-state visual evoked potentials. This method combines canonical correlation analysis, continuous wavelet transform, and support vector machine. The experimental results show that the algorithm achieved a classification accuracy of 91.76% and an information transmission rate of 48.92 bits per minute within 2 seconds, significantly improving the performance of the brain computer interface system for steady-state visual evoked potentials [12].

In summary, many scholars have conducted research on image segmentation and achieved certain results. However, the above research still has some limitations, such as using only a small dataset, which makes the model only perform well in specific datasets. Moreover, most scholars use a single algorithm model without improving the model, resulting in insufficient generalization ability of the model. This research

employs sinusoidal mapping and the simplex method to enhance CS and optimize the accuracy of optimization by utilizing sinusoidal adaptive probability of discovery. Additionally, it improves the clustering center by enhancing CS to address the issue of the FC algorithm's weaker global search ability and its sensitivity to noise. The FC algorithm's weak global search ability can be improved by optimizing the clustering center through improved CS. Additionally, introducing domain space information into the algorithm can optimize the objective function, which is necessary because the FC algorithm is more sensitive to noise.

III. RESEARCH ON IMAGE SEGMENTATION MODEL BASED ON FUZZY CLUSTERING AND CUCKOOBIRD OPTIMIZATION ALGORITHM

This section first analyzes the fuzzy clustering image segmentation algorithm and the cuckoo algorithm. In response to the weak global search ability of the fuzzy clustering algorithm, the cuckoo algorithm is improved to optimize the clustering center. Then, to address the issues of noise sensitivity and slow convergence speed in fuzzy clustering algorithms, neighborhood spatial information was introduced to improve the model, and an improved fuzzy clustering image segmentation algorithm with noise resistance was proposed.

A. IMPROVEMENT OF FUZZY CLUSTERING IMAGE SEGMENTATION ALGORITHM AND CUCKOO BIRD ALGORITHM

FC is a method of cluster analysis that, unlike traditional hard clustering methods, allows samples to belong to multiple cluster clusters rather than just one defined cluster. In FC, each sample has a certain degree of affiliation that indicates the degree to which it belongs to each cluster. Furthermore, Figure 1 depicts the process of clustering it [13].
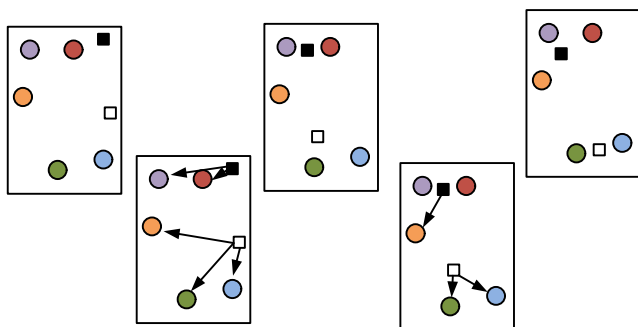

FIGURE 1. Clustering algorithm clustering process.

The fundamental idea behind FC is to optimize an objective function in order to ascertain each sample's degree of affiliation and clustering center; the fuzzy C-means algorithm (FCM) is the most widely used FC approach. The FCM algorithm introduces the concept of fuzziness, allowing each data point to belong to a different degree of clustering, thus better adapting to the situation of fuzzy data. The fuzzy C-means algorithm can divide samples into different

clustering clusters based on similarity. The basic idea of this algorithm is to determine the membership degree and clustering center of each sample by optimizing the objective function, and its expression is shown in equation (1).

$$J = \sum_{i=1}^{C} \sum_{j=1}^{N} u_{ij}^m d^2(x_j, v_i) \qquad (1)$$

In equation (1), u_{ij} denotes the degree of affiliation, d^2 denotes the Euclidean distance, x_j denotes the individual pixel points, C is the clusters, N is the total pixels, and m is the fuzziness index, v_i represents the clustering center of pixels. Up until the objective function reaches the minimal value, the affiliation matrix and clustering centers' values are updated continually in order to optimize the value of the objective function. At the end of the iteration, it is necessary to choose the appropriate termination conditions, there are generally two ways to choose the termination conditions, one is in accordance with the difference between the two iterations of the objective function before and after the relationship between the size of a certain threshold, although the running efficiency of the method has been improved, but it will fall into the situation of the local optimum. The other is in accordance with the difference between the pixel affiliation before and after two iterations and the relationship between the threshold value, the method is not as efficient as the first way, but its algorithmic accuracy is higher than the first. Therefore, in image processing, the pixels are categorized and divided by maximum affiliation, the expression is shown in equation (2).

$$k = \arg \max\{u_{ij}, i = 1, 2, \cdots, C\} \qquad (2)$$

In equation (2), C is the clusters and u_{ij} is the degree of affiliation. The IS process of FCM is shown in Figure 2.
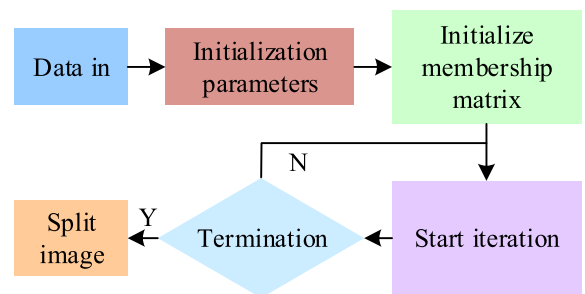

FIGURE 2. Flowchart of FCM algorithm.

In Figure 2, firstly, the image data is input, secondly, the parameters of the FCM algorithm model are initialized and the clustering center is determined, then the affiliation matrix is initialized under the constraints and the iteration starts. Every iteration, it is necessary to update its clustering center and affiliation matrix until the termination conditions are reached and the clustering results are output. Segmentation of the image is performed according to the principle of maximum affiliation. The pseudo-code of the fuzzy C-means algorithm is shown in Figure 3.

```
Pseudocode: Fuzzy C-Means Clustering Algorithm

1. Initialization
   for each data point in the dataset
      initialize membership degree for all clusters randomly
      ensure the sum of membership degrees for each point across all clusters equals 1
   select number of clusters C
   choose fuzziness coefficient m > 1 (usually 2)
   set termination threshold ε (a small positive number)
   initialize cluster centers V randomly or based on some heuristic
2. Membership Update
   repeat
      for each data point x_k
         for each cluster center v_i
            calculate the distance between x_k and v_i
            update membership degree u_ik using the formula:
            u_ik = 1 / sum_{j=1}^{C} ( (||x_k - v_i||) / (||x_k - v_j||) )^(2/(m-1))

3. Cluster Centers Update
   for each cluster center v_i
      update v_i using the formula:
      v_i = (sum_{k=1}^{N} u_ik^m * x_k) / sum_{k=1}^{N} u_ik^m

4. Termination Check
   if the maximum change in cluster centers is less than ε
      terminate the loop

5. Result Processing
   for each data point
      assign to cluster with the highest membership degree
   calculate final cluster centers
   store cluster labels for each data point for further analysis

# End of Algorithm
```

FIGURE 3. FCM pseudo-code.

The heuristic optimization technique known as CS was influenced by bird breeding behavior. Cuckoos deceive other birds by laying their offspring in their nests, thus realizing that the host bird helps them with tasks such as hatching and rearing their young. CS's fundamental goal is to optimize the search by simulating the birds' behaviors of searching for nests and taking away the eggs from other birds' nests, all of which are centered on the optimization problem to seek the optimal solution of the problem.

Finding the ideal position for a bird's nest is the most crucial stage in CS, and in general, higher-quality bird's nests serve as the primary selection objects. Levy flight (LF) strategy is extremely similar to the process of choosing the bird's nest; nevertheless, LF route features exhibit randomness and a higher global search capacity. The distribution law of LF is shown in equation (3).

$$Levy \sim u = t^{-\bar{\lambda}}, (1 \leq \bar{\lambda} \leq 3) \tag{3}$$

In equation (3), u is the step size and t is the number of generations. The distribution of the LF's probability density function is improved since it varies with time, as illustrated in equation (4).

$$S_L = \frac{\mu}{|v|^{1/\beta}}, (1 \leq \beta \leq 2) \tag{4}$$

In equation (4), S_L denotes the updated step size, and the distribution pattern of μ is $\mu \sim N(0, \delta_\mu^2)$, and the distribution pattern of v is $v \sim N(0, \delta_\mu^2)$. CS has several stipulations, the first one is that the cuckoos are randomly selected when they

make a choice of host nests, and lay only one egg at a time. Equation (5) displays the equation for the updating of the bird's nest location.

$$X_i^{t+1} = X_i^t + \alpha \oplus Levy(\lambda) \tag{5}$$

In equation (5), a denotes the control parameter of the step size, X denotes the bird's nest position, $\oplus$ denotes the term-by-term multiplication, and $Levy(\lambda)$ denotes the LF. The basic flow of CS under the three regulations is shown in Figure 4.

Firstly, Figure 4 initializes the location of the bird's nest. The value of each bird's nest placement to the goal function is then determined. Ultimately, the position of the bird's nest is determined by LF, and the fitness value (FV) of the original and present bird's nests is computed. Regardless of whether the original bird's nest's FV is higher than the current bird's nest's FV, the original bird's nest position is preserved and updated. The host bird adjusts its nest position by using Levy's flying when it finds the egg, and when the iteration meets the requirement, it produces the optimal adaption value. While CS offers certain benefits, such as superior robustness, great adaptive ability, and global search capability, it also has certain drawbacks. During the search process, CS may still end up at the local optimal solution even though it has the potential to search globally. Especially in cases where the solution space has a complex structure or there are multiple local optimal solutions, CS may not be able to jump out of the local optimal solutions efficiently. The convergence speed of CS may vary greatly from problem to problem. For some complex problems, the convergence speed of the algorithm may be slower, and more time and iterations are needed to find a satisfactory solution. And CS needs to set some parameters reasonably, and the flexibility of the algorithm will be greatly limited if the parameters are set fixedly. Different problems may require different parameter settings, which requires some experience and experiments to determine the best parameters. Finally, CS does not have a direct internal information sharing mechanism. The algorithm realizes the search process by adjusting the step size and position of cuckoos, and does not introduce information exchange between individuals in the population as other algorithms do. Therefore, it will cause information waste and the convergence speed in the later stage of the search will not be improved.

As a result, CS is enhanced, where the likelihood that bird eggs will be discovered and disposed of significantly affects the algorithm's overall convergence. And when the algorithm is iterated to a later stage, the fixed probability of discovery affects the search efficiency and accuracy of the model, which in turn leads to unsatisfactory results of the optimization search. Setting Pa starts to change with the number of iterations, as shown in equation (6).

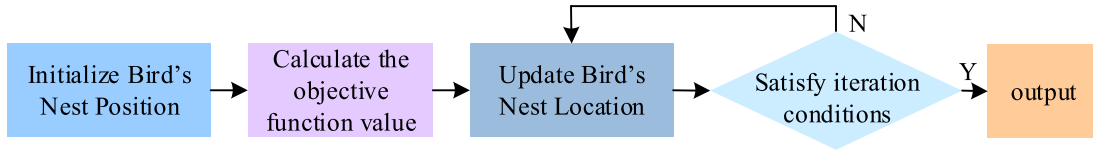$$P_a = P_a \cdot \sin\left(\frac{\pi}{2} + \frac{T_{iter\_now} - 1}{T_{iter\_\max} - 1}\right) \tag{6}$$

FIGURE 4. Basic flow of cuckoo search algorithm.

In equation (6), P_a is the probability that the host bird finds cuckoo eggs, *iter_now* is the current iterations, and *iter_max* A denotes the maximum iterations. Due to CS's few parameters and comparatively straightforward model implementation, it is common for the local optimal solution to be selected quickly during the optimization search process. Therefore, Sine mapping is used to optimize the optimization process of CS, and the Sine mapping is shown in equation (7).

$$Z_{K+1} = \frac{4}{a} \sin(\pi z_k) \tag{7}$$

In equation (7), the value domain of z_{k+1} is $[-1,1]$ and the value domain of a is $(0,4]$. In response to the slow convergence speed of the CS algorithm, the simplex method is introduced to improve the algorithm. The simplex method is an optimization algorithm used to solve linear programming problems, which aims to find a solution that maximizes the linear objective function under a set of linear constraints. Every time a new bird's nest is generated or its position is updated, the worst solution can be eliminated first using the simplex method, and then replaced by a new solution. The update process of the simplex method is shown in Figure 5.

In Figure 5, the basic idea of the simplex method is to start from an initial simplex and then iteratively move the vertices of the simplex in an attempt to find a better solution. These moves are achieved by searching around the vertices of the current simplex, changing the value of the decision variable to improve the value of the objective function. This process will continue to iterate until a solution that meets certain conditions is found. The improved cuckoo search (ICS) steps are shown in Figure 6.

As illustrated in Figure 6, each parameter is initialized first, followed by the position of the bird's nest being initialized and the adaption value of the nest being computed. After calculating the step size and using LF to update the bird's nest location, the unfavorable FV of the old bird's nest site is removed and the new bird's nest location is updated using the simplex approach. The location of the birdhouse is updated if its adaption value is higher than its previous location, and vice versa [14], [15]. After that, the optimal location is determined by sine mapping, the optimal location of the bird's nest is updated using sinusoidal adaptive discovery probability, and other parameters are output once the iteration reaches the maximum threshold.
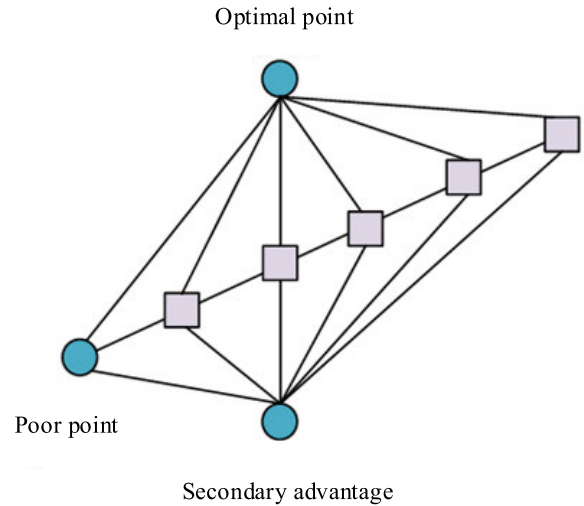

FIGURE 5. Update process of simplex method.

B. RESEARCH ON IMAGE SEGMENTATION MODEL BASED ON IMPROVED CUCKOO BIRD OPTIMIZATION ALGORITHM

The traditional FCM algorithm suffers from sensitivity to initial values, poor global convergence, and tends to fall into local optima. Therefore the improved CS and FCM algorithms are combined to discriminate the images. In the ICS-FCM algorithm, each cuckoo bird's nest is set as a set of clustering centers, and each clustering center serves as the basis for the division of the final IS [16], [17]. The initial population is formed by initializing N bird nests; equation (8) illustrates the coding of a bird nest.

$$X_{nest}(i) = (V_{i1}, V_{i2}, \cdots, V_{ij}, \cdots V_{ik}), i \in [1, N] \tag{8}$$

In equation (8), $X_{nest}(i)$ represents the clustering center and V_{ij} represents the image gray value. The indicator is taken by rand function combined with upper and lower bounds, and after repeating this operation N times, the cuckoo population is formed. The traditional CS finds the optimal solution by loop iteration, in FC algorithm, it is also evaluated by finding the optimal solution of the objective. Equation (9) displays the fitness function of the enhanced algorithm, ICS-FCM.

$$f = J(U, A) = \sum_{j=1}^{m} \sum_{i=1}^{n} \mu_{ij}^{c} d_{ij}^{2} \tag{9}$$

The fuzzy index is represented by c in equation (9), the Euclidean distance from the ith sample point to the
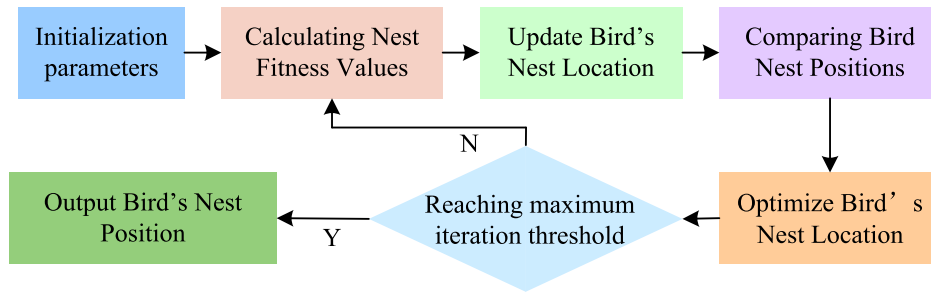
FIGURE 6. Improved cuckoo search flowchart.

jth clustering center is represented by d_{ij}, and the affiliation degree of the ith sample point belonging to the jth class is represented by μ_{ij}. The value of the new clustering center, or the position of the bird's nest, is produced by this method after each iteration. Figure 7 illustrates the precise flow of the revised algorithm.
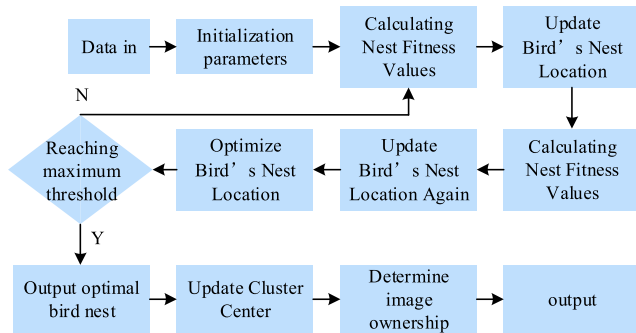

FIGURE 7. Flowchart of ICS-FCM algorithm.

Initializing the number of clusters, maximum number of iterations, chance of discovery, fuzzy index, and number of populations in Figure 7 involves first dividing and inputting the video of the soccer match into individual pictures. Secondly, N samples are randomly generated as the initial clustering center, i.e. bird's nest location, by rand function. Then, initialize the affiliation matrix, calculate the FV of each bird's nest using the fitness function, and compare the results to choose the best bird's nest [18], [19]. Next, the LF is used to update the bird's nest position, the simplex technique is used to eliminate the worse bird's nest position, and the FV of the new bird's nest is recalculated. If the FV of the new bird's nest is higher than that of the old bird's nest, the location and FV of the new bird's nest are modified appropriately. The ideal placement for the birdhouse is maintained while being updated by the sinusoidal adaptive discovery probability [20], [21], [22]. Use sine mapping to optimize the placement of the bird's nest. Then, compare the new nest's FV with the old one and move the nest if it is in a better place. Until the iterations surpasses the predefined value, the nest's position, the optimal FV, and other details are output [23], [24], [25]. To get the final pixel attribution and produce the IS result, update the affiliation matrix and clustering center based on the best position for the bird's nest.

Upon resolving the issues with initial value sensitivity, inadequate global convergence, and susceptibility to local optimization inherent in the conventional FCM algorithm, it is discovered that increased noise levels substantially impact the image's information content and result in subpar performance of the IS effect at the end. When segmenting the image, the spatial information is taken into account by minimizing the optimization objective function, as indicated by equation (10), as opposed to the typical FC technique which does not take this into account [26], [27].

$$J = \sum_{j=1}^{m} \sum_{k=1}^{n} u_{jk}^2 d_{jk}^2 \qquad (10)$$

In equation (10), u_{jk} denotes the affiliation degree and d_{jk}^2 denotes the Euclidean distance. Because the clustering centers generated by the FCM technique are randomly generated, it is quite easy to end up in the local optimal solution while doing the iterative optimization search. And the algorithm also does not consider the pixel space information, which causes the FCM algorithm to be easily affected by noise, thus affecting the segmentation results. The FCM approach for IS will significantly improve the model's mis-classification if the neighborhood space information is supplied. Equation (11) illustrates the enhanced objective function [28], [29].

$$J_{FCM-S} = \sum_{i=1}^{N} \sum_{k=1}^{C} \mu_{ki}^m \left(\|x_i - v_k\|^2 + \frac{\alpha}{N_R} \sum_{x_j \in N_j} \|x_j - v_k\|^2 \right) \qquad (11)$$

In equation (11), μ_{ki} represents the FC affiliation of the ith pixel in the center of the k class clustering, N_R represents the membership degree of all data points in the dataset. α represents the influence parameter of the domain point on the current pixel point. The setting size of this parameter has a very close connection with the segmentation effect, too small a parameter value will make the algorithm too sensitive to noise, and too large a parameter value will make the segmentation effect too vague [30], [31]. Therefore, it is necessary to update the value of the parameter in real time, but this situation will lead to the algorithm is too inefficient.

The improved objective function is shown in equation (12).

$$J = \sum_{i=1}^{C} \sum_{k=1}^{N} \mu_{ik}^m \|x_k - v_i\|^2 + \alpha \sum_{i=1}^{C} \sum_{k=1}^{N} \mu_{ik}^m \|\overline{x}_k - v_i\|^2 \tag{12}$$

In equation (12), μ_{ki} represents the FC affiliation of the ith pixel point in the center of the kth class clustering, and α represents the image parameter of the domain point to the current pixel point. This objective function is replaced with that of the original CS and optimized, and the optimized algorithm is named ICS-FCM-S1, and the specific steps of this algorithm are shown in Figure 8.
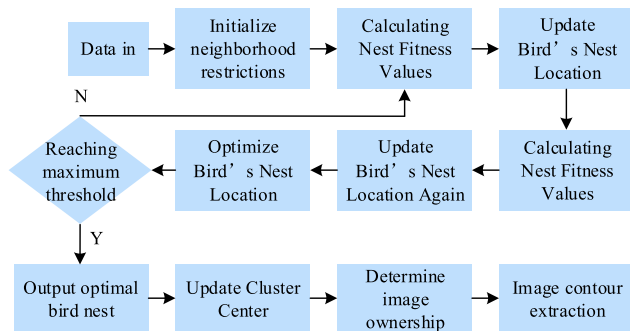

FIGURE 8. Flowchart of ICS-FCM-S algorithm.

In Figure 8, firstly, the video of the soccer match is inputted and divided into pictures to initialize the clusters, the maximum iterations, the probability of discovery, the fuzzy index, the number of clusters, the domain restriction parameter and the number of populations. Then N samples are randomly generated as the initial clustering center, i.e., the bird's nest location, by rand function. Following the initialization of the affiliation matrix, each bird's nest's FV is determined using the fitness function, and the best bird's nest is identified by comparing the FVs of each bird's nest [32], [33], [34]. Next, the LF is used to update the bird's nest position, the simplex technique is used to eliminate the worse bird's nest position, and the FV of the new bird's nest is recalculated. When comparing the new bird's nest FV to that of the previous bird's nest, if the new bird's nest FV is higher, the bird's nest location and FV are adjusted accordingly. Maintain the ideal position for the bird's nest while updating it based on a sinusoidal adaptive discovery probability. The birdhouse location is optimized by sine mapping, the obtained birdhouse FV is compared with the previous one and if the new birdhouse has better FV, then the birdhouse location is changed. The location of the bird's nest, the optimal FV, and other information are output until the iterations exceeds the predetermined value. Referencing the affiliation, remove the section of interest using the active contour approach, update the affiliation matrix and clustering center based on the best place for the bird's nest to ascertain the pixel's ultimate belonging, and then output the IS result.

IV. PERFORMANCE ANALYSIS OF IMAGE SEGMENTATION MODEL BASED ON FUZZY CLUSTERING AND CUCKOO OPTIMIZATION ALGORITHM

The first section of this chapter introduces several common algorithms and compares their fitness, convergence accuracy and processing time in Quartic function and Sphere function respectively. The second chapter analyzes the performance of the model through fuzzy partition effect, cluster partition coefficient and cluster partition entropy.

A. IMPROVED CUCKOO SEARCH PERFORMANCE ANALYSIS

MATLAB R2022 is used in this experiment, the operating system is Windows 10, and the CUP is Intel Core i7-4710MQ processor with 2.5GHz and 8.00G of RAM. The dataset adopts the SoccerNet dataset, which is a large-scale dataset for understanding and analyzing football videos, developed in collaboration with the academic and industrial communities in Europe. The SoccerNet dataset can provide rich football
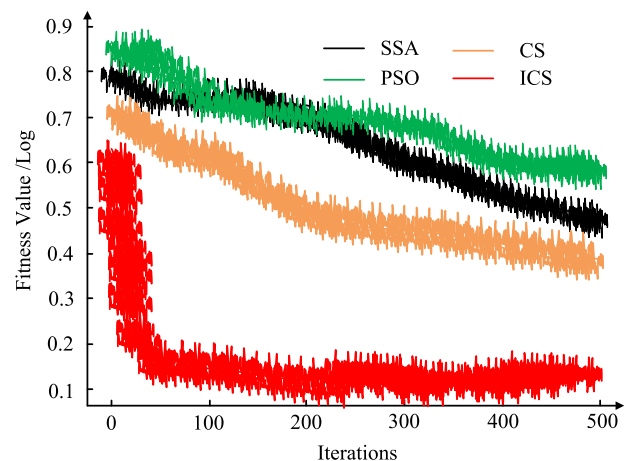
(a)Sphere function fitness change curve
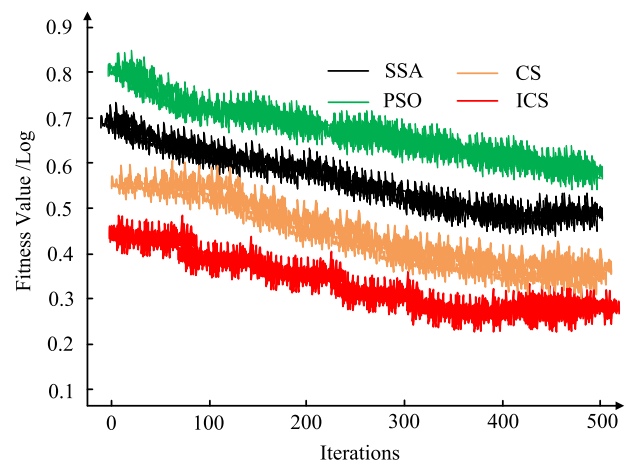
(b)Quartic function fitness change curve

FIGURE 9. Variation curves of the fitness of the four algorithms in different functions.

match videos with detailed annotations and tags. In order to validate the performance of this ICS, Sparrow Search Algorithm (SSA) and Particle Swarm Optimization (PSO) are introduced to compare with this proposed algorithm, Quartic function and Sphere function are selected to compare the fitness change curves under different algorithms respectively. Furthermore, Figure 9 presents the findings.

The number of iterations is the horizontal coordinate in Figure 9, and the log10, the bottom logarithm, is the vertical coordinate. The fitness of the Quartic function for the four algorithms is represented by Figure 9(b), whereas the fitness of the Sphere function for the four algorithms is represented by Figure9(a). As the number of iterations grows in Figure 9(a), the value of fitness increases in the Sphere function. And the ICS model tends to stabilize and reaches the maximum value when the iteration here reaches about 50. In Figure 9(b), in the Quartic function, the FV is getting larger with the increase of iteration number, but it is more gentle, and the FV of each algorithm does not change much, but the proposed ICS has the largest FV among the four methods. The outcomes revealed that the proposed ICS exhibits better global optimization ability among the four methods. The more concentrated the cluster, the better the performance.
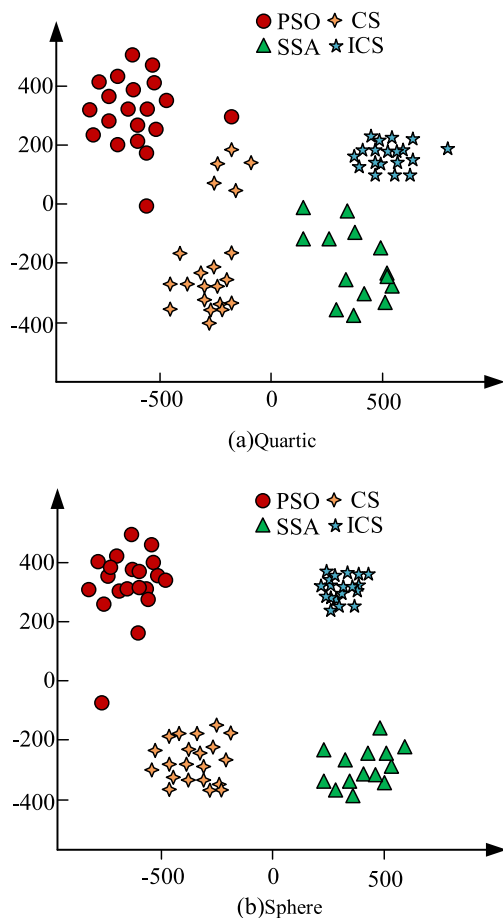
To further validate that the proposed method is able to select the best clusters, the clustering effect of each algorithmic model is added to the manuscript as an evaluation metric to analyze the performance of the model. The clustering effects of the four methods were analyzed, and the results are shown in Figure 10.

Figure 10(a) shows the clustering performance of each algorithm model in the Quartic function, while Figure 10(b) shows the clustering performance of each algorithm model in the Sphere function. From Figure 10, it can be seen that among various algorithm models, the PSO algorithm Mo model has the worst clustering effect, while the ICS algorithm model has the best clustering effect. The convergence accuracies of the four methods are compared in Sphere function and Quartic function, and the results are shown in Figure11.
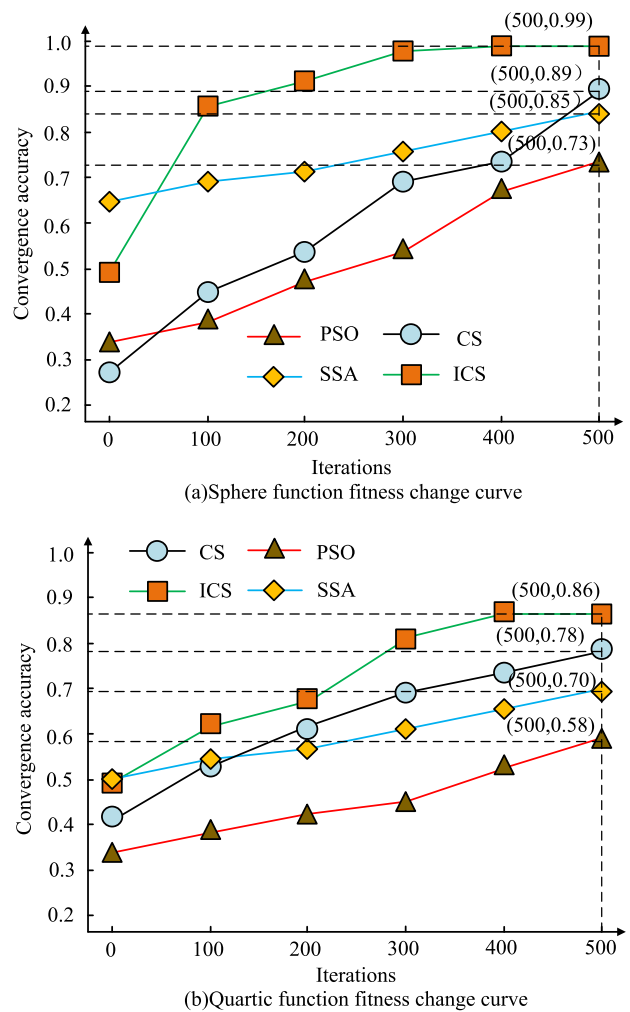

(a)Quartic

(b)Sphere

FIGURE 10. Convergence accuracy of the four algorithms in different functions.

(a)Sphere function fitness change curve

(b)Quartic function fitness change curve

FIGURE 11. Convergence accuracy of the four algorithms in different functions.

Figure 11(a) illustrates the Sphere function's convergence accuracy for the four algorithms, whereas Figure 11(b) shows the Quartic function's convergence accuracy for the same set of algorithms. As the iterations increases, each algorithm's convergence accuracy in the Sphere function increases in
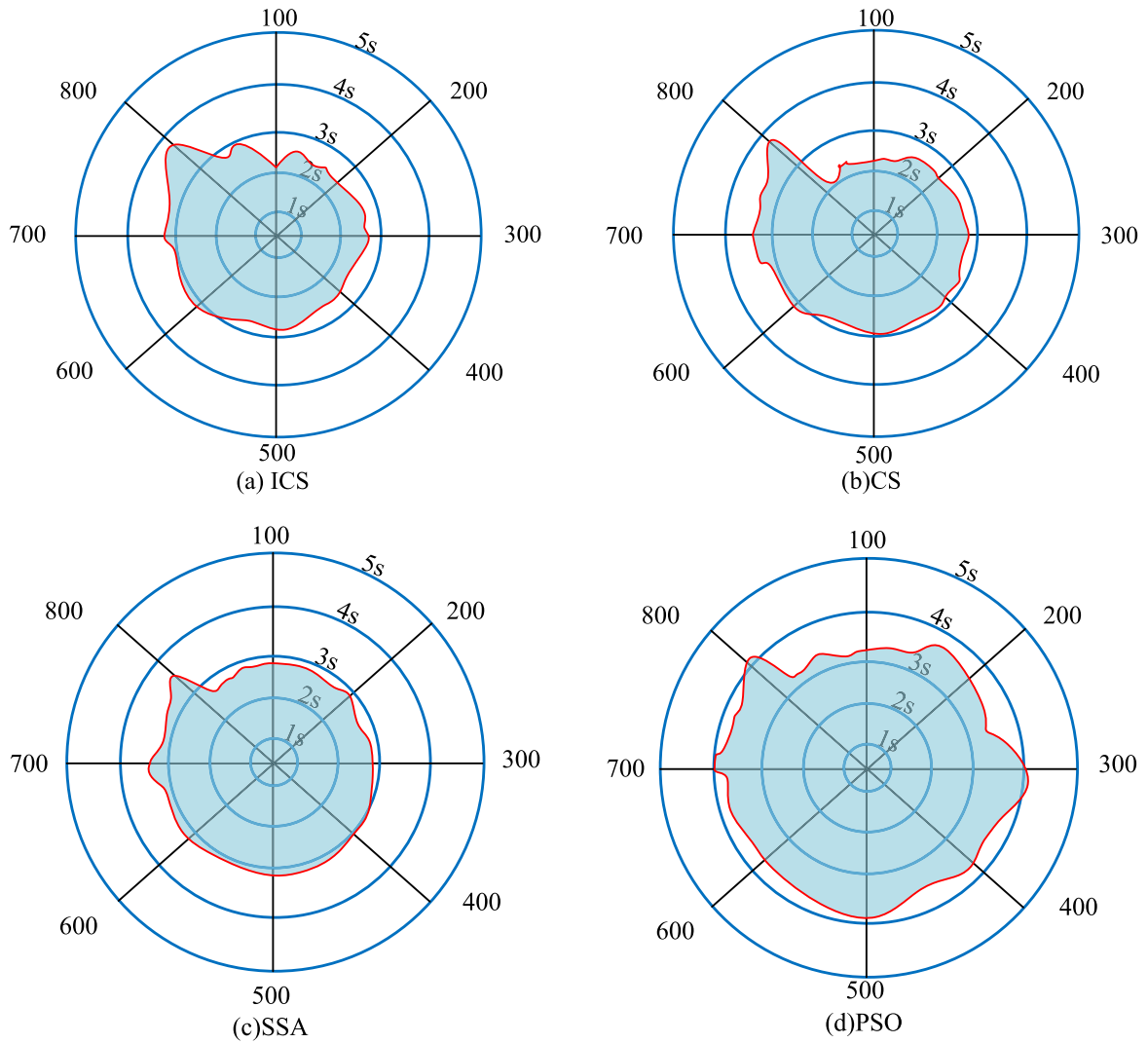
FIGURE 12. Processing time of the algorithm with different number of iterations.

Figure 11(a). ICS is the only algorithm that can achieve a high convergence accuracy with a low iterations, and when the iterations reaches 500, the convergence accuracy of ICS, CS, SSA, and PSO are, respectively, 0.99, 0.89, 0.85, and 0.73. In Figure 11(b), the convergence accuracy of each algorithmic model in Quartic function increases with the iterations. When the iterations reaches 500, the convergence accuracy of ICS, CS, SSA, and PSO are 0.86, 0.78, 0.70, and 0.58, respectively. The outcomes illustrate that, in comparison to the other four approaches, the ICS algorithm has higher convergence accuracy and faster convergence rates. Figure 12 presents the comparison of the computing efficiency of the four algorithms at varying iteration counts.

From Figure 12, the time taken by the ICS algorithm for 100-500 iterations is 1.4s, 2.2s, 2.8s, 2.9s, and 3.0s. The time taken by the CS algorithm for 100-500 iterations is 1.8s, 2.7s, 2.8s, 3.2s, and 3.4s. The time taken by the SSA algorithm for 100-500 iterations is 2.1s, 2.9s, 3.1s, 3.5s, 3.6s, and 3.6s,

TABLE 1. Model scoring scale.

/	Group 1	Group 2	Group 3	Group 4	Group 5	References
ICS	89.2	93.5	84.2	86.9	84.5	This study
CS	85.7	87.6	83.4	79.5	81.6	This study
SSA	78.6	81.2	76.8	74.2	78.6	[35]
PSO	74.1	75.4	72.5	71.6	76.9	[36]

respectively. s, 3.1s, 3.5s, 3.6s. The time used by the PSO algorithm for 100-500 iterations is 2.2s, 3.1s, 3.5s, 3.7s, 3.8s. The experimental findings demonstrate that, out of the four algorithms, the suggested ICS algorithm uses less time for iterations. To test the suggested four methods, fifty testers were chosen at random and split into five equal groups. The findings are displayed in Table 1.

As shown in Table 1, the five subgroups scored 89.2, 93.5, 84.2, 86.9, and 84.5 for ICS. The five subgroups scored 85.7, 87.6, 83.4, 79.5, and 81.6 for CS. The five subgroups scored 78.6, 81.2, 76.8, 74.2, and 78.6 for SSA. The five subgroups scored 74.1, 75.4, 72.5, 71.6, and 76.9 for PSO. were 74.1, 75.4, 72.5, 71.6, and 76.9, respectively. The outcomes illustrate that the suggested ICS performs better in every model and has a high level of superiority, suggesting that the testers are aware of the ICS.

## B. PERFORMANCE ANALYSIS OF IMAGE SEGMENTATION MODEL BASED ON IMPROVED CUCKOO OPTIMIZATION ALGORITHM

To verify the effectiveness of the proposed improved algorithm, the experimental dataset used Wyscout's publicly available dataset, the Socket match event dataset. Randomly select 3 videos from the dataset, and divide each video into 500 slices. Video 1 and Video 2 are used as the training set, and Video 3 is used as the validation set. The FCM algorithm model, CS-FCM algorithm model, and ICS-FCM algorithm model are introduced and compared with the proposed method. The fuzzy partitioning effects of the four methods are shown in Figure 13.

The division effect of various algorithms in the dataset of video 1 is represented by Figure 13(a), and the division effect of various algorithms in the dataset of video 2 is represented by Figure 13(b). In Figure 13(a), in the dataset formed by Video 1, the division effect of each algorithm rises with the increase of the training set, and when the size of the dataset is 800, the division effect of ICS-FCM-S1 algorithmic model, ICS-FCM algorithmic model, CS-FCM algorithmic model, and FCM algorithmic model are 0.82, 0.88, 0.90, and 0.97, respectively. As can be seen from Figure 13(b), in the dataset formed by Video 2, the division effect of each algorithm rises as the training set increases. When the size of the dataset is 800, the division effects of the ICS-FCM-S1 algorithm model, ICS-FCM algorithm model, CS-FCM algorithm model, and FCM algorithm model are 0.80, 0.72, 0.70, and 0.61, respectively. According to the experimental results, out of the four models, the suggested ICS-FCM-S1 algorithm model has the best division effect and better convergence in the video 1 produced dataset. Six representative soccer actions in the dataset are selected: upside down golden hook, powerful pump shot, rainbow cross, Marseille slalom and v-pull, and these five actions are named as actions 1 to 5. Cluster division coefficients and cluster division entropy are introduced to evaluate the model, and the results are shown in Figure 14.

Figure 14(a) compares the segmentation coefficients of the four methods for various action photos, whereas Figure 14(b) compares the segmentation entropy of the four algorithms for various action images. In Figure 14(a), the division coefficients of the ICS-FCM-S1 algorithm model for the five actions are 0.88, 0.87, 0.87, 0.79, and 0.81, respectively. The division coefficients of the proposed ICS-FCM-S1 algorithm model are the largest among the four algorithms.
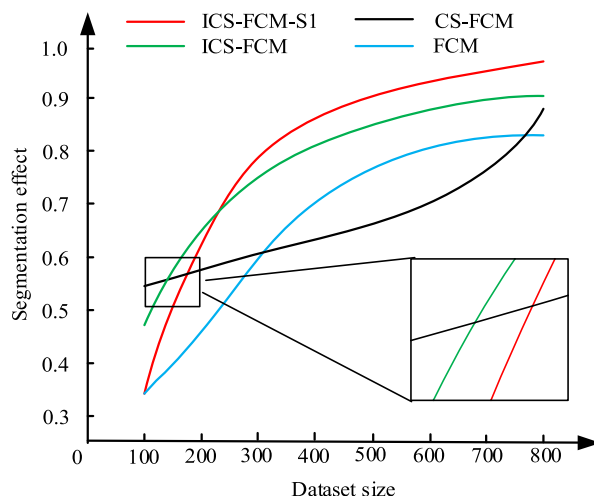
(a) Different Algorithm Partitioning Effects in Video 1 Dataset
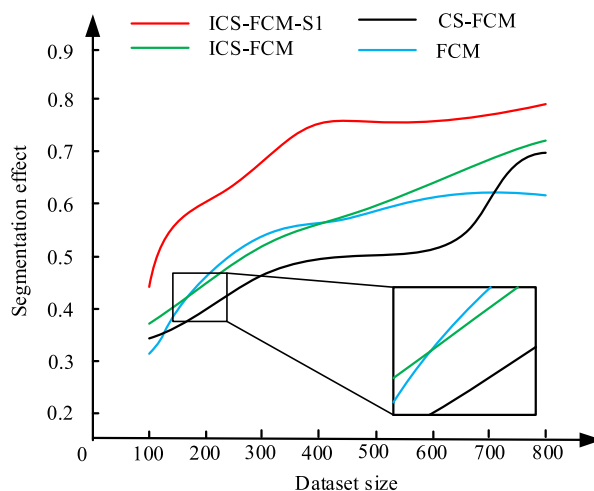
(b) Different Algorithm Partitioning Effects in Video 2 Dataset

FIGURE 13. Comparison of the segmentation effect of the four algorithms in different datasets.

From Figure 14(b), the division entropy of the ICS-FCM-S1 algorithm model for the five actions is 0.35, 0.34, 0.41, 0.40, 0.32, respectively. Among the four algorithms, the division entropy of the proposed ICS-FCM-S1 algorithm model is the smallest. According to the experimental findings, the ICS-FCM-S1 algorithm model performs better since it has bigger division coefficients and lower division entropy. The computing times of the four approaches are compared across several datasets, and the findings are displayed in Figure 15.

Figure 15(a) shows the time comparison of each algorithm in the dataset composed of football video 1 and video 2, while Figure 15(b) shows the time comparison of each algorithm in the dataset composed of football video 3. As shown in Figure 15(a), in the datasets formed by Video 1 and Video 2, when the dataset is small, the processing time of the ICS-FCM-S1 algorithm model remains basically unchanged. The processing time of the algorithm model is 2.0s, 1.4s, 1.1s,
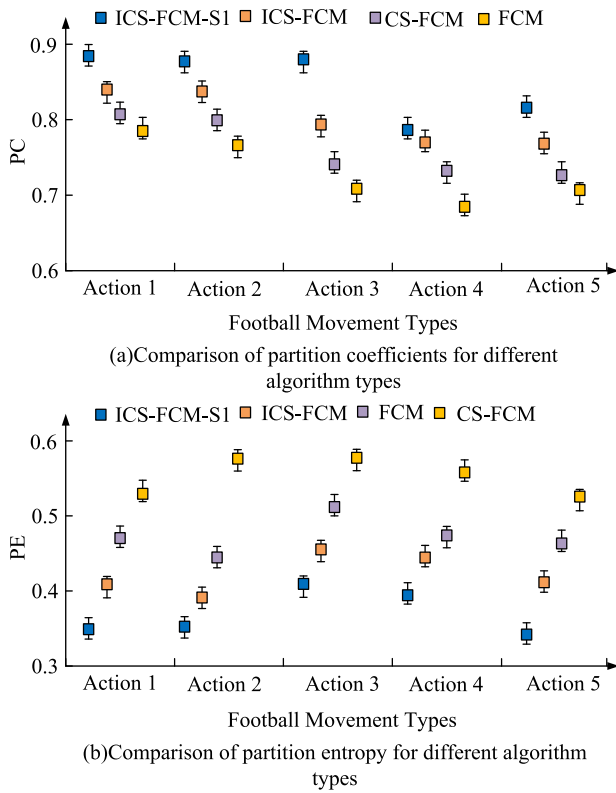
(a)Comparison of partition coefficients for different algorithm types

(b)Comparison of partition entropy for different algorithm types

FIGURE 14. Comparison of division coefficients and division entropy of four algorithms.

TABLE 2. Ablation experiment.

Model	P	R	ACC	F1	mAP	Loss
ICS	0.84	0.71	82.41%	0.82	0.81	0.82
FCM	0.87	0.76	85.62%	0.85	0.83	0.11
FCM-S1	0.87	0.76	86.34%	0.91	0.79	0.076
ICS-FCM	0.88	0.78	87.65%	0.93	0.88	0.067
ICS-FCM-S1	0.89	0.82	88.97%	0.94	0.93	0.064

and 1.0s respectively when the dataset size is 100, 200, 400, and 800. In Figure 15(b), the processing time of the ICS-FCM-S1 algorithm model in the dataset formed by Video 3 is 0.9s, 1.0s, 1.9s and 2.1s for the dataset sizes of 100, 200, 400, and 800, respectively. The outcomes revealed that the proposed algorithm has a lower processing time and a higher processing efficiency among the four methods. To verify the performance of each algorithm, ablation experiments were conducted to analyze the performance of the model. The results are shown in Table 2.

According to Table 2, it can be seen that after adding the ICS algorithm model, the ICS-FCM algorithm model has a significant improvement compared to the FCM algorithm model, and after adding neighborhood spatial information. The FCM-S1 algorithm model also has significant improvements compared to the FCM algorithm model. The ablation
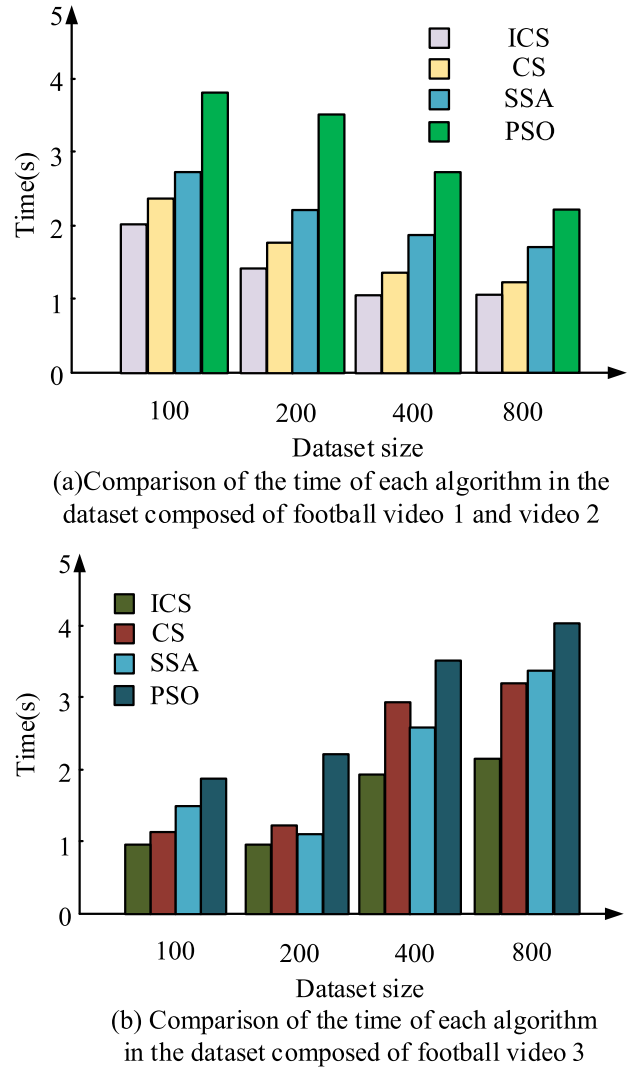

(a)Comparison of the time of each algorithm in the dataset composed of football video 1 and video 2

(b) Comparison of the time of each algorithm in the dataset composed of football video 3

FIGURE 15. Comparison of processing time of each algorithm in different data.

TABLE 3. Athlete evaluation form.

/	Group 1	Group 2	Group 3	Group 4	Group 5
ICS-FCM-S1	87.2	98.2	82.2	89.9	82.5
ICS-FCM	81.7	92.4	78.4	84.6	80.6
CS-FCM	76.6	87.1	74.2	81.1	75.6
FCM	73.5	81.5	71.3	77.4	72.6

experiment shows that the ICS algorithm model used and the optimization of neighborhood spatial information can greatly improve the performance of the model. Twenty soccer players were randomly selected and divided into five groups and allowed to rate the four models. Table 3 presents the findings.

As shown in Table 3, the five groups scored 87.2, 98.2, 82.2, 89.9, and 82.5 for ICS-FCM-S1. 81.7, 92.4, 78.4, 84.6 and 80.6 for ICS-FCM. 76.6, 87.1, 74.2, 81.1 and 75.6 for CS-FCM. 73.5, 81.5, 71.3, 77.4 and 72.6 for FCM scores were 73.5, 81.5, 71.3, 77.4 and 72.6, respectively. The

outcomes of the trial demonstrated that the suggested algorithmic model performed better in every model and received high marks from the athletes.

V. CONCLUSION

The use of artificial intelligence technology has led to the widespread adoption of machine learning and cluster analysis methods for match discrimination. This study proposes an improved FCIS algorithm with noise immunity that accurately segments images in match videos. The findings of the study indicated that for the dataset consisting of video 2, with a dataset size of 800, the ICS-FCM-S1 algorithmic model had the highest segmentation effect of 0.80, followed by the ICS-FCM algorithmic model with a segmentation effect of 0.72, the CS-FCM algorithmic model with a segmentation effect of 0.70, and the FCM algorithmic model with a segmentation effect of 0.61. When the iterations reached 500 in the Quartic function, the convergence accuracies of ICS, CS, SSA, and PSO were 0.86, 0.78, 0.70, and 0.58, respectively. In the dataset formed by Video 2, the convergence accuracies of the ICS-FCM-S1 algorithm model, the ICS-FCM algorithm model, the CS-FCM algorithm model, and the FCM algorithm models were 0.80, 0.72, 0.70, and 0.61, respectively, when the size of the dataset was 800. Five soccer actions were randomly selected and segmented. The division coefficients for the five actions were 0.88, 0.87, 0.87, 0.79, and 0.81, while the division entropies were 0.35, 0.34, 0.41, 0.40, and 0.32. The division entropies of the ICS-FCM-S1 algorithmic model for the five actions were 0.35, 0.34, 0.41, 0.40, and 0.32. The ICS-FCM-S1 algorithmic model processes datasets of size 100, 200, 400, and 800 in 1.0s, 1.1s, 1.4s, and 2.0s, respectively. The outcomes of the experiment indicated that the proposed algorithmic model effectively segments images to aid in discriminating soccer matches. However, this research has some deficiencies. The proposed method does not establish an information sharing mechanism between populations, rendering the information before and after unreferenced. Additionally, the convergence accuracy and speed of the algorithm can be further improved.

REFERENCES

[1] R. Palanikumar, K. Ramasamy, and P. S. Ragavan, "Faulty node detection and recovery scheme for large-scale wireless sensor network using hosted cuckoo optimization algorithm," *Int. J. Commun. Syst.*, vol. 35, no. 9, pp. 1–20, Mar. 2022, doi: 10.1002/dac.5143.

[2] M. Braik, A. Sheta, H. Al-Hiary, and S. Aljahdali, "Enhanced cuckoo search algorithm for industrial winding process modeling," *J. Intell. Manuf.*, vol. 34, no. 4, pp. 1911–1940, Apr. 2023, doi: 10.1007/s10845-021-01900-1.

[3] M. M. Woldeamanuel, T. Kim, S. Cho, and H.-K. Kim, "Estimation of concrete strength using thermography integrated with deep-learning-based image segmentation: Case studies and economic analysis," *Expert Syst. Appl.*, vol. 213, Mar. 2023, Art. no. 119249, doi: 10.1016/j.eswa.2022.119249.

[4] J. Fan, M. Du, L. Liu, G. Li, D. Wang, and S. Liu, "Macerals particle characteristics analysis of tar-rich coal in northern Shaanxi based on image segmentation models via the U-Net variants and image feature extraction," *Fuel*, vol. 341, Jun. 2023, Art. no. 127757, doi: 10.1016/j.fuel.2023.127757.

[5] B. Ostdiek, A. D. Rivero, and C. Dvorkin, "Extracting the subhalo mass function from strong lens images with image segmentation," *Astrophysical J.*, vol. 927, no. 1, p. 83, Mar. 2022, doi: 10.3847/1538-4357/ac2d8d.

[6] A. Kumar, A. Kumar, A. Vishwakarma, and H. Lee, "An improved segmentation technique for multilevel thresholding of crop image using cuckoo search algorithm based on recursive minimum cross entropy," *IET Signal Process.*, vol. 16, no. 6, pp. 630–649, Aug. 2022, doi: 10.1049/sil2.12148.

[7] G. Xiang and X. Xiang, "3D trajectory optimization of the slender body freely falling through water using cuckoo search algorithm," *Ocean Eng.*, vol. 235, Sep. 2021, Art. no. 109354, doi: 10.1016/j.oceaneng.2021.109354.

[8] D. K. Anguraj, K. Thirugnanasambandam, R. S. Raghav, S. V. Sudha, and D. Saravanan, "Enriched cluster head selection using augmented bifold cuckoo search algorithm for edge-based Internet of Medical Things," *Int. J. Commun. Syst.*, vol. 34, no. 9, pp. 1–13, Apr. 2021, doi: 10.1002/dac.4817.

[9] L.-W. Wang, Z.-S. Liu, W.-C. Siu, and D. P. K. Lun, "Lightening network for low-light image enhancement," *IEEE Trans. Image Process.*, vol. 29, pp. 7984–7996, 2020, doi: 10.1109/TIP.2020.3008396.

[10] W. Zhang, Z. Li, H.-H. Sun, Q. Zhang, P. Zhuang, and C. Li, "SSTNet: Spatial, spectral, and texture aware attention network using hyperspectral image for corn variety identification," *IEEE Geosci. Remote Sens. Lett.*, vol. 19, pp. 1–5, 2022, doi: 10.1109/LGRS.2022.3225215.

[11] A. K. Bhandari, B. Subramani, and M. Veluchamy, "Multi-exposure optimized contrast and brightness balance color image enhancement," *Digit. Signal Process.*, vol. 123, Apr. 2022, Art. no. 103406, doi: 10.1016/j.dsp.2022.103406.

[12] P. Ma, C. Dong, R. Lin, S. Ma, T. Jia, X. Chen, Z. Xiao, and Y. Qi, "A classification algorithm of an SSVEP brain–computer interface based on CCA fusion wavelet coefficients," *J. Neurosci. Methods*, vol. 371, Apr. 2022, Art. no. 109502, doi: 10.1016/j.jneumeth.2022.109502.

[13] A. Das, A. Namtirtha, and A. Dutta, "Fuzzy clustering of acute lymphoblastic leukemia images assisted by eagle strategy and morphological reconstruction," *Knowl.-Based Syst.*, vol. 239, Mar. 2022, Art. no. 108008, doi: 10.1016/j.knosys.2021.108008.

[14] D. Toresa, F. Wiza, A. A. Irwanda, W. S. Abiyus, E. Edriyansyah, and T. Taslim, "The cuckoo optimization algorithm enhanced visualization of morphological features of diabetic retinopathy," *J. Appl. Eng. Technol. Sci. (JAETS)*, vol. 4, no. 2, pp. 929–939, Jun. 2023, doi: 10.37385/jaets.v4i2.1978.

[15] H. Zavieh, A. Javadpour, Y. Li, F. Ja'fari, S. H. Nasseri, and A. S. Rostami, "Task processing optimization using cuckoo particle swarm (CPS) algorithm in cloud computing infrastructure," *Cluster Comput.*, vol. 26, no. 1, pp. 745–769, Feb. 2023, doi: 10.1007/s10586-022-03796-9.

[16] B. Joshi and M. K. Thakur, "Genetic algorithm- and cuckoo search algorithm-based routing optimizations in network-on-chip," *Arabian J. Sci. Eng.*, vol. 48, no. 8, pp. 9635–9644, Aug. 2023, doi: 10.1007/s13369-022-07272-9.

[17] K. Thirugnanasambandam, U. Prabu, D. Saravanan, D. K. Anguraj, and R. S. Raghav, "Fortified cuckoo search algorithm on training multi-layer perceptron for solving classification problems," *Pers. Ubiquitous Comput.*, vol. 27, no. 3, pp. 1039–1049, Mar. 2023, doi: 10.1007/s00779-023-01716-1.

[18] X. Yang, X. Hao, T. Yang, Y. Li, Y. Zhang, and J. Wang, "Elite-guided multi-objective cuckoo search algorithm based on crossover operation and information enhancement," *Soft Comput.*, vol. 27, no. 8, pp. 4761–4778, Apr. 2023, doi: 10.1007/s00500-022-07605-8.

[19] C. Liu, J. Wang, L. Zhou, and A. Rezaeipanah, "Solving the multi-objective problem of IoT service placement in fog computing using cuckoo search algorithm," *Neural Process. Lett.*, vol. 54, no. 3, pp. 1823–1854, Jan. 2022, doi: 10.1007/s11063-021-10708-2.

[20] J. Liang, "Value analysis and realization of artistic intervention in rural revitalization based on the fuzzy clustering algorithm," *Sci. Program.*, vol. 2022, pp. 1–9, Jan. 2022, doi: 10.1155/2022/3107440.

[21] C. Zhao, Y. Zhang, Y. Xue, and T. Niu, "Encryption transmission verification method of IT operation and maintenance data based on fuzzy clustering analysis," *Mobile Netw. Appl.*, vol. 27, no. 4, pp. 1386–1396, Apr. 2022, doi: 10.1007/s11036-022-01919-5.

[22] S. Wang, S. Xiao, W. Zhu, and Y. Guo, "Multi-view fuzzy clustering of deep random walk and sparse low-rank embedding," *Inf. Sci.*, vol. 586, pp. 224–238, Mar. 2022, doi: 10.1016/j.ins.2021.11.075.

[23] M. Gheisari, H. Hamidpour, Y. Liu, P. Saedi, A. Raza, A. Jalili, H. Rokhsati, and R. Amin, "Data mining techniques for web mining: A survey," *Artif. Intell. Appl.*, vol. 1, no. 1, pp. 3–10, Oct. 2022, doi: 10.47852/bonviewaia2202290.

[24] Y.-T. Li, J.-Z. Li, L. Ren, K. Xu, S. Chen, L. Han, H. Liu, X.-L. Guo, D.-L. Yu, D.-H. Li, L. Ding, L.-M. Peng, and T.-L. Ren, "Light-controlled reconfigurable optical synapse based on carbon nanotubes/2D perovskite heterostructure for image recognition," *ACS Appl. Mater. Interfaces*, vol. 14, no. 24, pp. 28221–28229, Jun. 2022, doi: 10.1021/acsami.2c05818.

[25] K. Bhosle and V. Musande, "Evaluation of deep learning CNN model for recognition of Devanagari digit," *Artif. Intell. Appl.*, vol. 1, no. 2, pp. 114–118, Feb. 2023, doi: 10.47852/bonviewaia3202441.

[26] A. Olamat, P. Ozel, and S. Atasever, "Deep learning methods for multi-channel EEG-based emotion recognition," *Int. J. Neural Syst.*, vol. 32, no. 5, pp. 225–232, Apr. 2022, doi: 10.1142/s0129065722500216.

[27] C. C. Liu, S. G. Hajra, S. D. Fickling, G. Pawlowski, X. Song, and R. C. N. D'Arcy, "Novel signal processing technique for capture and isolation of blink-related oscillations using a low-density electrode array for bedside evaluation of consciousness," *IEEE Trans. Biomed. Eng.*, vol. 67, no. 2, pp. 453–463, Feb. 2020, doi: 10.1109/TBME.2019.2915185.

[28] S. Phadikar, N. Sinha, and R. Ghosh, "Automatic EEG eyeblink artefact identification and removal technique using independent component analysis in combination with support vector machines and denoising autoencoder," *IET Signal Process.*, vol. 14, no. 6, pp. 396–405, Aug. 2020, doi: 10.1049/iet-spr.2020.0025.

[29] Q. He and S. Pursiainen, "An extended application 'Brain Q' processing EEG and MEG data of finger stimulation extended from 'Zeffiro' based on machine learning and signal processing," *Cogn. Syst. Res.*, vol. 69, pp. 50–66, Oct. 2021, doi: 10.1016/j.cogsys.2020.08.006.

[30] Q. Lin, S. Song, I. D. Castro, H. Jiang, M. Konijnenburg, R. van Wegberg, D. Biswas, S. Stanzione, W. Sijbers, C. Van Hoof, F. Tavernier, and N. Van Helleputte, "Wearable multiple modality bio-signal recording and processing on chip: A review," *IEEE Sensors J.*, vol. 21, no. 2, pp. 1108–1123, Jan. 2021, doi: 10.1109/JSEN.2020.3016115.

[31] Q. Zhu, L. Gao, H. Song, and Q. Mao, "Learning to disentangle emotion factors for facial expression recognition in the wild," *Int. J. Intell. Syst.*, vol. 36, no. 6, pp. 2511–2527, Feb. 2021, doi: 10.1002/int.22391.

[32] N. B. Kar, D. R. Nayak, K. S. Babu, and Y. Zhang, "A hybrid feature descriptor with Jaya optimised least squares SVM for facial expression recognition," *IET Image Process.*, vol. 15, no. 7, pp. 1471–1483, Jan. 2021, doi: 10.1049/ipr2.12118.

[33] X. Jin and Z. Jin, "MiniExpNet: A small and effective facial expression recognition network based on facial local regions," *Neurocomputing*, vol. 462, pp. 353–364, Oct. 2021, doi: 10.1016/j.neucom.2021.07.079.

[34] R. Zhi, C. Zhou, T. Li, S. Liu, and Y. Jin, "Action unit analysis enhanced facial expression recognition by deep neural network evolution," *Neurocomputing*, vol. 425, pp. 135–148, Feb. 2021, doi: 10.1016/j.neucom.2020.03.036.

[35] M. K. Dutta, M. Kaur, and R. K. Sarkar, "Comparative performance analysis of fuzzy logic and particle swarm optimization (PSO) techniques for image quality improvement: With special emphasis to old and distorted folk paintings," *Optik*, vol. 254, Mar. 2022, Art. no. 168644, doi: 10.1016/j.ijleo.2022.168644.

[36] A. Priyanka and K. Ganesan, "Radiomic features based severity prediction in dementia MR images using hybrid SSA-PSO optimizer and multiclass SVM classifier," *IRBM*, vol. 43, no. 6, pp. 549–560, Dec. 2022, doi: 10.1016/j.irbm.2022.05.003.

TING WANG was born in Tieling, Liaoning, in August 1980. He received the bachelor's degree in physical education, the master's degree in physical education and training, and the Ph.D. degree in sports science and theory of exercise training from Shanxi University, in 2002, 2008, and 2015, respectively.

From 2002 to 2017, he was an Assistant Researcher with Shanxi Institute of Sports Science. Since 2017, he has been an Associate Professor with the School of Physical Education, Shanxi University. He has published eight academic articles and presided more than six scientific research projects.

JINGLONG GENG was born in Baoding, Hebei, in May 1989. He received the bachelor's degree in sports training from Shanxi University Sports College, in 2007, the master's degree in physical education and training from the Capital University of Physical Education and Sports, in 2014, and the Ph.D. degree in physical education from South Korea's Woosuk University, in 2023.

Since 2014, he has been a Lecturer with the Physical Education College, Taiyuan Normal University. He has published more than ten academic articles, participated in four scientific research projects, and edited two books. His research interests include physical education and training.

JING WANG was born in Tianjin, in January 1988. She received the bachelor's degree in sports training and the master's degree in physical education and training from the Capital University of Physical Education and Sports, in 2010 and 2014, respectively, and the Ph.D. degree in physical education from Woosuk University, South Korea, in 2023, with a focus on research direction in physical education and training.

From September 2016 to November 2023, she was a Lecturer with Xinzhou Teachers University. Since 2023, she has been a Lecturer with Shanxi Vocational University of Engineering Science and Technology.

XIAO YAN was born in Taiyuan, Shanxi, in November 1993. She received the bachelor's degree in physical education from Shanxi Normal University, in 2017, and the master's degree in physical education with the School of Physical Education, Shanxi University, major in theory of exercise training, where she is currently pursuing the Ph.D. degree.

Since 2018, she has been a Scientific Researcher with Chinese Archery Team. She has published three academic articles.

• • •